Formation of brown carbon via reactions of ammonia with secondary organic aerosols from biogenic and anthropogenic precursors

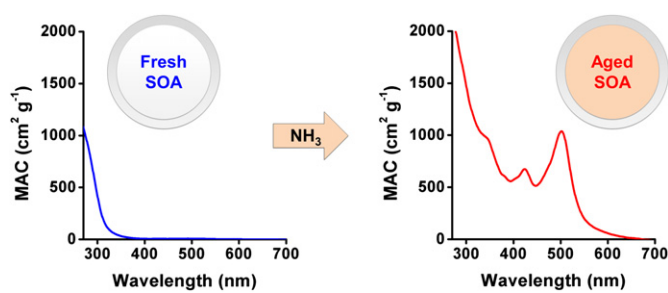Katelyn M. Updyke, Tran B. Nguyen [1], Sergey A. Nizkorodov*

Department of Chemistry, University of California, Irvine, CA 92697, USA

HIGHLIGHTS

► Secondary organic aerosols change color from white to brown in presence of ammonia.
► Browning reaction occurs for a wide range of biogenic and anthropogenic aerosols.
► Aqueous reaction with ammonium ion is equally efficient in producing brown carbon.
► The mass absorption coefficient is comparable to that of biomass burning aerosols.
► Secondary brown carbon may contribute to absorption of solar radiation by aerosols.

GRAPHICAL ABSTRACT

ABSTRACT

Filter samples of secondary organic aerosols (SOA) generated from the ozone (O_3)- and hydroxyl radical (OH)-initiated oxidation of various biogenic (isoprene, α-pinene, limonene, α-cedrene, α-humulene, farnesene, pine leaf essential oils, cedar leaf essential oils) and anthropogenic (tetradecane, 1,3,5-trimethylbenzene, naphthalene) precursors were exposed to humid air containing approximately 100 ppb of gaseous ammonia (NH_3). Reactions of SOA compounds with NH_3 resulted in production of light-absorbing "brown carbon" compounds, with the extent of browning ranging from no observable change (isoprene SOA) to visible change in color (limonene SOA). The aqueous phase reactions with dissolved ammonium (NH_4^+) salts, such as ammonium sulfate, were equally efficient in producing brown carbon. Wavelength-dependent mass absorption coefficients (MAC) of the aged SOA were quantified by extracting known amounts of SOA material in methanol and recording its UV/Vis absorption spectra. For a given precursor, the OH-generated SOA had systematically lower MAC compared to the O_3-generated SOA. The highest MAC values, for brown carbon from SOA resulting from O_3 oxidation of limonene and sesquiterpenes, were comparable to MAC values for biomass burning particles but considerably smaller than MAC values for black carbon aerosols. The NH_3/NH_4^+ + SOA brown carbon aerosol may contribute to aerosol optical density in regions with elevated concentrations of NH_3 or ammonium sulfate and high photochemical activity.

1. Introduction

Atmospheric aerosols affect the average surface temperatures on both global and local scales (Solomon et al., 2007). On average, aerosols cool the climate by directly scattering solar radiation and

* Corresponding author. Tel.: +1 949 824 1262.
  E-mail address: nizkorod@uci.edu (S.A. Nizkorodov).
[1] Current address: Department of Geological and Planetary Sciences, California Institute of Technology, Pasadena, CA 91125, USA.

indirectly through aerosol–cloud interactions. Certain types of aerosols are also capable of absorbing visible solar radiation and warming the lower atmosphere. Brown carbon (Alexander et al., 2008; Andreae and Gelencser, 2006; Bond and Bergstrom, 2006; Ramanathan et al., 2007), black carbon (Bond and Bergstrom, 2006; Haywood and Boucher, 2000), and mineral dust (Usher et al., 2003) are the major known types of light-absorbing aerosols.

Conventional wisdom associates light-absorbing organic aerosol (OA) with primary sources and light-scattering OA with secondary sources. Known examples of primary brown carbon sources are smoldering forest fires and residential coal combustion (Alexander et al., 2008; Andreae and Gelencser, 2006; Bond and Bergstrom, 2006). However, recent experiments demonstrated that secondary sources of brown carbon may also exist, with light-absorbing compounds being produced directly in the atmosphere via multi-phase reactions between gas-phase, particulate-phase and cloud micro-droplet constituents. Examples include the reactions of OH radicals with aromatic hydroxy-acids and phenols in cloud water (Chang and Thompson, 2010; Gelencser et al., 2003; Hoffer et al., 2004), aqueous reactions of glyoxal and methylglyoxal with ammonium sulfate (AS, $(NH_4)_2SO_4$) (Galloway et al., 2009; Noziere et al., 2009; Sareen et al., 2010; Shapiro et al., 2009; Yu et al., 2011), gas-to-particle uptake of glyoxal by deliquesced AS aerosol (Trainic et al., 2011), aqueous reactions between glyoxal and amino acids (De Haan et al., 2009), reactions of limonene SOA with ammonia (NH_3) (Laskin et al., 2010) and with AS (Bones et al., 2010; Nguyen et al., 2012), heterogeneous reactions of gaseous isoprene on acidic aerosol particles (Limbeck et al., 2003), and aqueous photo-chemistry of pyruvic acid in the presence of common atmospheric electrolytes (Rincon et al., 2009, 2010). Light-absorbing compounds can also form as a result of acid-catalyzed aldol condensation of volatile aldehydes (Casale et al., 2007; Esteve and Noziere, 2005; Garland et al., 2006; Krizner et al., 2009; Noziere and Esteve, 2005; Noziere et al., 2006; Noziere and Esteve, 2007; Zhao et al., 2005) and nitration of polycyclic aromatic hydrocarbons (Jacobson, 1999; Kwamena and Abbatt, 2008; Pitts et al., 1978). For example, filter samples of secondary organic aerosols (SOA) generated from aromatic precursors under high-NO_x conditions are visibly brown in color (Jaoui et al., 2008).

Recent work (Bones et al., 2010; Laskin et al., 2010; Nguyen et al., 2012) on SOA produced by O_3-initiated oxidation of limonene demonstrated that this type of SOA undergoes browning during exposure to reduced nitrogen compounds such as $NH_3(g)$, NH_4^+ (from dissolved AS or other ammonium salts), and amino acids. Browning took place on a time scale of hours when aqueous extracts of SOA were mixed with AS or amino acids over an environmentally-relevant range of pH values (pH = 4–8) (Bones et al., 2010). Active removal of water by evaporation of solutions containing limonene SOA and AS or amino acids greatly accelerated the browning process, suggesting that browning involves condensation reactions between ammonium and carbonyls (Nguyen et al., 2012). Similar reactions occurred when limonene SOA particles were exposed to NH_3 vapor in humid air (Laskin et al., 2010). Bones et al. (2010) also examined browning in aqueous reactions between AS and SOA formed by the O_3-initiated oxidation of several other monoterpenes (α-pinene, β-pinene, β-myrcene, γ-terpinene) and isoprene. The extent of browning, as well as the resulting absorption spectra, varied greatly amongst these SOA, suggesting that the NH_4^+-mediated browning chemistry requires rather specific types of organic compounds in the aerosol. Fluorescence spectroscopy, absorption spectroscopy, and high-resolution mass spectrometry experiments determined that the chromophores are likely to be conjugated nitrogen-containing species (Bones et al., 2010; Laskin et al., 2010; Nguyen et al., 2012).

The mass absorption coefficient, MAC ($cm^2 g^{-1}$), is a useful parameter for assessing the effect of light-absorbing aerosols on climate. MAC is directly proportional to the absorption coefficient α_{air} (Mm^{-1}) for air containing a certain mass concentration of particles C_{PM} ($\mu g\ m^{-3}$).

$$\alpha_{air}(\lambda) = MAC(\lambda) \times C_{PM} \times 10^{-4} \tag{1}$$

Strictly speaking, the quantity we are calling MAC is the bulk absorption coefficient normalized by the concentration of the organic material in SOA; it should not be confused with mass-absorption cross section used in studies of light absorption and scattering by individual particles. Nguyen et al. (2012) quantified MAC over the UV and visible wavelength range for the organic material produced by evaporation of aqueous mixtures of limonene + O_3 SOA with AS, glycine, and various inorganic acids. MAC values for other types of SOA aged with reduced nitrogen species are currently unknown. The goal of this work is to determine the ability of SOA to form brown carbon compounds from exposure to gaseous NH_3. We examine different types of SOA formed from O_3- and OH-initiated oxidation of biogenic and anthropogenic precursors. In each case, we determine the extent of browning by quantifying MAC of the resulting brown carbon material. The MAC values measured here suggest that brown carbon produced by this mechanism may contribute to the aerosol absorption, especially in areas that have high emissions of NH_3 or dissolved ammonium salts, and are not strongly affected by primary black and brown carbon emissions from fires and fossil fuel combustion.

2. Materials and methods

2.1. Preparation of different types of model SOA

Both O_3-initiated and OH-initiated oxidation was used to prepare model SOA from suitable volatile organic compounds (VOC). For the VOC + O_3 reactions, a 3.5 SLM (standard liters per minute) flow of oxygen (99.994% purity) was sent through an O_3 generator, a home-built O_3 photometric detector, and a 17 L glass flow tube reactor (Bones et al., 2010). The reactor was maintained at <2% relative humidity (RH), 750 ± 50 mbar pressure, and 20–24 °C temperature. Liquid VOC were injected into the air flow using a syringe pump at a rate ranging from 15 to 20 $\mu L\ h^{-1}$. In the absence of O_3, the estimated steady-state mixing ratio of VOC in the flow tube was ~10 ppm (parts per million by volume). O_3 was added in excess with mixing ratios ranging from 20 to 80 ppm. Although the mixing ratios of VOC and O_3 were high relative to typical ambient values, the flow tube residence time was less than 5 min. We previously demonstrated (Bateman et al., 2011; Walser et al., 2008) using high resolution mass spectrometry that the limonene + O_3 SOA formed in the flow tube is similar in composition to that formed in a smog chamber under much lower (<0.1 ppm) mixing ratios. A 1-m long charcoal denuder removed more than 99% residual O_3 from the flow exiting the reactor. SOA was collected on PTFE filters (Millipore fluoropore, 0.2 μm pore size), which were pre-weighed with a Sartorius ME-5F filter balance (1 μg precision). After the collection, the filters were weighed again. The collection time (1–3 h) was chosen so that filters contained 500–1000 μg of SOA material at the end of the preparation.

The VOC + OH reactions were conducted in a 5 m^3 Teflon chamber equipped with UV-B lights similarly to the procedure described by Nguyen et al. (2011a). Experiments were performed under dry conditions (RH < 2%) with 2 ppm of H_2O_2 as an OH precursor (added by evaporating a 30% H_2O_2 solution in water,

Table 1

Types of SOA samples examined in this work. The three-letter abbreviations next to the precursor names are used to refer to SOA in the text. SOA from O_3-initiated oxidation such as LIM/O_3 were prepared in a flow tube, while SOA from OH-initiated oxidation such as TMB/OH/NO_x were prepared in a smog chamber. The initial VOC and NO mixing ratios are listed only for the chamber-generated aerosol. $\langle\Delta MAC\rangle$ is the 300–700 nm wavelength-averaged change in MAC induced by the exposure of SOA to gaseous NH_3 compared to fresh samples that were not aged. The peak value of ΔMAC (or a value at 500 nm if there is no well-defined peak) is given in the last column.

Precursor (abbreviated name)	Oxidant	Initial VOC (ppb)	Initial NO (ppb)	Reaction time (h)	Collection time (h)	Amount collected (µg)	$\langle\Delta MAC\rangle$ ($cm^2\ g^{-1}$)	ΔMAC peak value ($cm^2\ g^{-1}$)
Limonene (LIM)	O_3	–	–	1.3	2	2000	400	1200
LIM	OH	250	<1	2	4	1000	170	80
α-Cedrene (CED)	O_3	–	–	2.3	2	200	260	700
α-Humulene (HUM)	O_3	–	–	2.3	2	700	300	800
Farnesene (FAR)	O_3	–	–	2.3	2	500	60	10
α-Pinene (PIN)	O_3	–	–	1.3	2	1000	50	50
PIN	OH	250	<1	2	4	700	100	40
Pine Needle Oil (PNO)	O_3	–	–	2.3	2	800	100	60
Cedar Leaf Oil (CLO)	O_3	–	–	2.3	2	400	500	1000
Isoprene (ISO)	OH	250	–	2	4	100	50	20
ISO	O_3	–	–	1.3	2	800	10	5
Tetradecane (TET)	OH	250	–	2	4	900	80	60
1,3,5-trimethylbenzene (TMB)	OH	250	<1	2	4	1000	20	40
TMB	OH	250	300	2	4	800	70	10
Naphthalene (NAP)	OH	100	<1	2	4	1000	200	100
NAP	OH	100	300	2	4	1000	1000	400

Fisher Scientific). For high-NO_x experiments, 300 ppb (parts per billion by volume) of NO was also added. Depending on specific VOC, initial VOC mixing ratios were either 100 or 250 ppb (Table 1). After mixing, UV-B lights were turned on to initiate the photooxidation. A scanning mobility particle sizer (SMPS) was used to monitor the particle size and number distribution. Typical mass concentrations after 2 h of photooxidation were 60–500 µg m^{-3}. After 2 h of photooxidation the lights were turned off and SOA was collected through an activated carbon denuder at 30 SLM using PTFE filters. Typically the collection lasted for 3 h and 200–1000 µg were collected per filter sample. For select experiments, SOA was collected by impaction on clean foil substrates using a multi-orifice uniform-deposit impactor (MOUDI, MSP model 110-R) sampling at 30 SLM. The largest mass of SOA material (20–300 µg after 4 h) was typically collected on stages 8 (0.18–0.32 µm) or 9 (0.10–0.18 µm).

The types of SOA examined in this work are listed in Table 1, and the structures and commercial sources of single-component SOA precursors are listed in Table S1 of the Supplementary material section. O_3-derived SOA include the oxidation products of isoprene, terpenes (α-pinene, limonene), sesquiterpenes (α-cedrene, α-humulene, farnesene) and essential oils (pine leaf oil and cedar leaf oil). OH-derived SOA include the oxidation of isoprene, monoterpenes (limonene, α-pinene) and select anthropogenic precursors (tetradecane, 1,3,5-trimethylbenzene, naphthalene). For the anthropogenic precursors, we examined both high-NO_x and low-NO_x oxidation conditions. This selection of SOA and oxidation conditions is representative of both remote and urban atmospheric environments. Hereinafter, we refer to specific SOA samples by precursor name (shortened to three-letter codes introduced in Table 1) and oxidant (O_3, OH, and NO_x) used. For example, limonene + O_3 SOA are labeled LIM/O_3, and high-NO_x 1,3,5-trimethylbenzene + OH SOA are labeled TMB/OH/NO_x. We use abbreviations such as VOC/O_3 to collectively refer to all SOA produced by the same method.

2.2. Aging and UV/Vis measurements

A polystyrene Petri dish (9.2 cm diameter, 1.5 cm height) was filled with 50 mL of 0.1 M ammonium nitrate (NH_4NO_3) stock solution. Estimated headspace volume in the aging chamber was 50 cm^3. The equilibrium concentrations of gases in the headspace volume were estimated with AIM-II model (Clegg et al., 1998) as

100 ppb for NH_3, 0.2 ppt for HNO_3, and 99.7 %RH for water vapor. We note that HNO_3 did not play any part in the aging process, therefore, any salt of ammonium would work just as well. For example, aging above a 0.1 M $(NH_4)_2SO_4$ solution, which has negligible equilibrium vapor pressure of H_2SO_4 but comparable equilibrium vapor pressure of NH_3, produced similar results. However, the presence of water vapor likely played a significant role because the aging reactions between NH_3/NH_4^+ with SOA carbonyls likely occurred in the aqueous layer on SOA. It is unlikely that these reactions would occur under very dry conditions when the amount of absorbed water in aerosols is too small to maintain acid-base equilibria. The SOA filter was placed on a polystyrene cap (5.5 cm diameter, 0.5 cm height) above the NH_4NO_3 solution, without physical contact, to be exposed to humid NH_3 vapors. A larger Petri dish was used to cover the filter and solution, and sealed with paraffin tape. The samples were allowed to "age" in the dark for a desired period of time, typically 72 h. Identically prepared fresh SOA samples were vacuum-sealed and stored in the freezer for the same amount of time. Control SOA samples were also prepared using the same methods, and aged using a Petri dish filled with 50 mL of pure water. No browning was observed for either fresh or control samples. The aged and fresh samples were extracted from the filter using a suitable solvent (methanol for most experiments; water for experiments evaluating the fraction of water-soluble material in the samples) with 20 min sonication. The resulting SOA extracts were filtered with 0.2 µm syringe filters. In some experiments, a secondary extraction was performed to confirm that the primary extraction was complete.

The filtered extracts were placed in a 1 cm quartz cuvette for absorption measurements. UV/Vis absorption spectra were taken with a dual-beam spectrometer (Shimadzu UV-2450) using pure solvent as reference. The extent of SOA browning was quantified in terms of effective mass absorption coefficient (MAC) of the organic material. Wavelength-dependent MAC (cm^2 g^{-1}) can be directly calculated (Chen and Bond, 2010) from the base-10 absorbance A_{10} of an SOA extract with solution mass concentration C_{mass} (g cm^{-3}) measured over pathlength b (cm):

$$MAC(\lambda) = \frac{A_{10}^{solution}(\lambda) \times \ln(10)}{b \times C_{mass}} \qquad (2)$$

We note that this equation is only valid in situations when the dissolution does not change the chemical identity of the

chromophores via solvolysis and other solvent-induced reactions. As there was no evidence of solvolysis of the chromophores in our samples following the dissolution, we can assume that this method faithfully captures the absorption properties of the aged SOA material. In order to compare light-absorbing properties of different SOA, we will also use $\langle MAC \rangle$ averaged over the 300–700 nm region of the spectrum:

$$\langle MAC \rangle = \frac{1}{(700-300)\ nm} \times \int\limits_{300\ nm}^{700\ nm} MAC(\lambda)d\lambda \qquad (3)$$

Quantification of MAC using Eqs. (2) and (3) requires the SOA material to be fully extracted from the filter. In the previous studies of LIM/O_3 browning (Bones et al., 2010; Laskin et al., 2010; Nguyen et al., 2012), we used water as the extracting solvent. However, SOA made from sesquiterpenes, essential oils, tetradecane, and aromatics are not fully extractable in water. For example, the absorbance of the methanol extracts from CED/O_3 is much higher than that of the water extract (Fig. S1 in the Supplementary material section). In contrast, LIM/O_3 is extracted equally well by methanol and water (Fig. S2). We verified the completeness of extraction by methanol by performing a secondary extraction from the same filter (Fig. S3). Although methanol tends to convert a fraction of carboxylic acids and carbonyls into esters and hemiacetals, respectively (Bateman et al., 2008), this is not expected to significantly affect the appearance of visible spectra of SOA extracts. Indeed, the absorption spectra for water- and methanol-extracted LIM/O_3 in Fig. S2 are similar. We therefore adopted methanol as the solvent for all experiments in this manuscript. We note that Chen and Bond (2010) also used methanol for quantification of MAC in extracts of biomass-burning organic aerosol.

3. Results

The SOA-loaded filters that were not exposed to $\sim$100 ppb gaseous NH_3 remained unchanged in their visual appearance. The exposed SOA materials changed in color to different extents. The largest color change was observed for SOA produced by O_3-initiated oxidation of some biogenic precursors LIM, CED, HUM, PNO, and CLO. All of these samples were initially white and acquired a red-brown color after the exposure. However, other biogenic SOA samples such as FAR/O_3, PIN/O_3 and ISO/O_3 did not visibly brown even after prolonged chemical aging. These results are in agreement with Bones et al. (2010), who observed formation of brown carbon compounds in aqueous reactions of AS with dissolved LIM/O_3 but not with PIN/O_3 and ISO/O_3. OH-generated SOA samples also exhibited different degrees of browning, generally less than O_3-generated SOA samples. ISO/OH, PIN/OH and TET/OH remained white after aging. LIM/OH acquired a red-brown hue, but to a smaller extent than aged LIM/O_3. Initially-white TMB/OH and TMB/OH/NO_x developed a pale beige color. NAP/OH and NAP/OH/NO_x samples were yellow to begin with, and their color became more saturated after aging.

The preceding description is qualitative because the visual perception of sample's color strongly depends of the amount of SOA on the filter, which varied by an order of magnitude between different SOA (Table 1). MAC is a more quantitative measure of the degree of browning. Fig. 1 illustrates the effect of NH_3 exposure on the MAC values in three different types of SOA samples. The fresh CLO/O_3 SOA sample, representative of some of the biogenic SOA (Fig. 1A), had negligible absorbance over the visible range of the
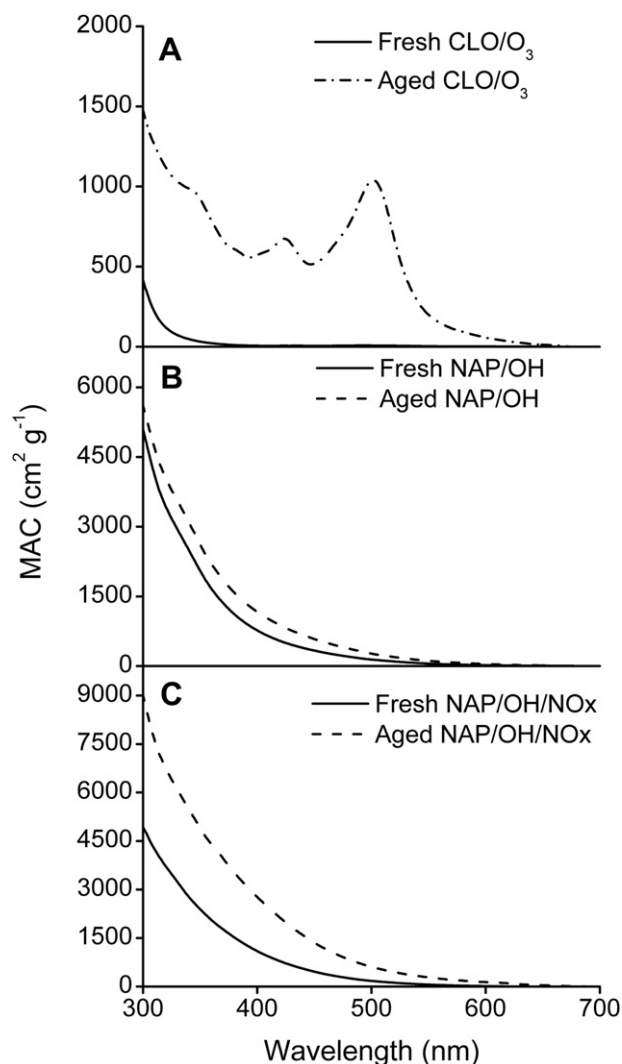
Fig. 1. Examples of absorption spectra of SOA extracts before and after aging. The dashed lines correspond to UV/Vis absorption spectra of SOA after exposure to gas phase NH_3; the solid lines are the spectra of the fresh samples. (A) The behavior of CLO/O_3 is representative of some of the biogenic SOA samples: negligible absorption of visible radiation in the fresh samples; well defined absorption bands in the aged samples. (B) NAP/OH and (C) NAP/OH/NO_x absorb visible radiation in both fresh and aged state, with the absorption increasing upon aging. Absorbances were converted to MAC using Eq. (2).

spectrum, consistent with its white color. A large absorption band at $\sim$500 nm with a MAC peak value of $\sim 10^3$ cm^2 g^{-1} appeared in the spectrum of the aged CLO/O_3 SOA, along with broad absorption below 500 nm.

NAP/OH (Fig. 1B) and NAP/OH/NO_x (Fig. 1C) were different from the rest of the SOA samples in that they had significant MAC at visible wavelengths even before aging. The absorption spectra of the freshly prepared SOA samples smoothly decayed from the UV into the visible range. In the wavelength range of 400–630 nm, MAC values for NAP-based SOA followed the usual power dependence on wavelength, $MAC(\lambda) = MAC_0 \times \lambda^{-AE}$, with the Ångström exponents (AE) of the order of 6.5. Exposure to NH_3 increased the MAC values across the entire wavelength range; the increase was larger for the NAP/OH/NO_x sample. AE of the aged NAP/OH and NAP/OH/NO_x SOA were of the order 6.2 and 6.7, respectively. There were no well-defined absorption bands as in the case of aged SOA from the biogenic precursors.

To isolate the change in MAC due to the NH_3-induced aging, it is convenient to define the difference in MAC between the aged and fresh samples:

$$\Delta MAC(\lambda) = MAC_{aged}(\lambda) - MAC_{fresh}(\lambda) \qquad (4)$$

Table 1 lists the peak values in ΔMAC for each SOA (or the ΔMAC value at $\lambda = 500$ nm if there is no well defined peak), as well as the 300–700 nm wavelength-averaged values of ΔMAC. The wavelength dependence of ΔMAC is shown in Figs. 2 and 3 for all the SOA studied in this work. In order to simplify comparison between different SOA types, we sorted the data between different panels in Figs. 2 and 3 by the conditions under which SOA was prepared.

We want to emphasize that aging by $NH_3(g)$ is not a unique mechanism of SOA browning. This reaction occurs with dissolved ammonium salts in an aqueous solution just as efficiently. For example, Fig. 4 compares ΔMAC values for LIM/O_3 SOA resulting from three different aging mechanisms: by exposure to $NH_3(g)$ for 3 days, by aqueous reaction with AS for 3 days, and by evaporation of an aqueous solution of SOA mixed with AS (the evaporation process takes just a few minutes; further details of the evaporative aging are provided by Nguyen et al. (2012)). The wavelength dependence and the absolute magnitudes of ΔMAC are similar in all three cases.

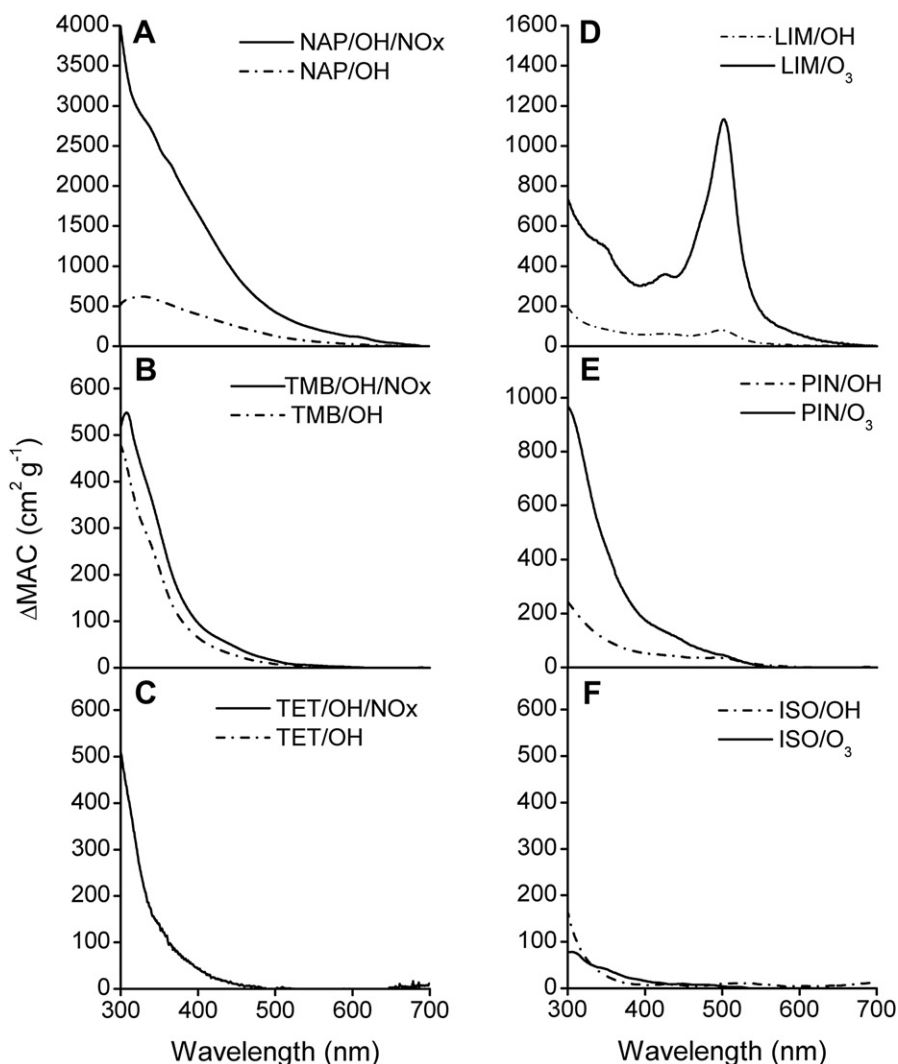Fig. 3. ΔMAC resulting from aging with NH_3 for select biogenic VOC/O_3 SOA.

Fig. 2. ΔMAC induced by aging with NH_3, which is attributable to secondary brown carbon. Comparisons are shown for aerosols prepared under high-NO_x vs. low-NO_x conditions (panels A–C) and OH vs. O_3 oxidation (panels D–F).
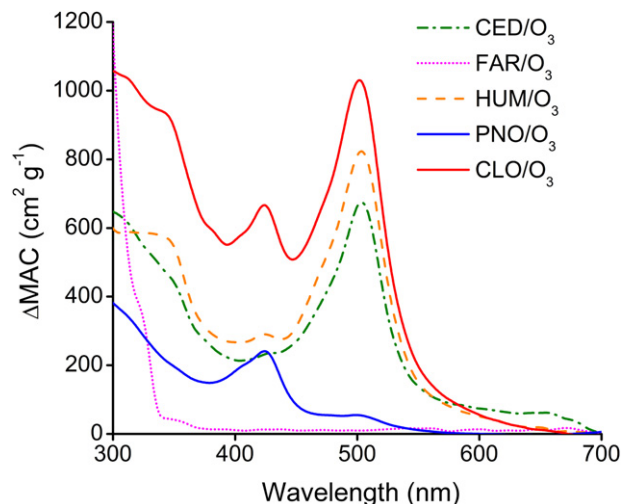
To emphasize that similar types of browning processes occur regardless of what form ammonia is in, we will refer to the aged aerosol as NH_3/NH_4^+ + SOA in further discussion.

Additional experiments and data consistency tests were performed; they are described in detail in the Supplementary material section and summarized briefly in this paragraph. In our studies, we determined that MAC values did not depend on the type of substrate on which SOA was collected (PTFE vs. foil substrates (Fig. S4)), which suggests that browning reactions were specific to the SOA material. We also verified that browning was not due to the reactions of impurities in the VOC precursors. The absorption spectra for the aged LIM/O_3 SOA were the same regardless of whether the limonene precursor was used as is or after extensive purification (Fig. S5). The main challenge of these experiments was the extended time it took to reach saturation in the extent of browning. In some cases, the measured MAC values continued to increase even after 4 days of NH_3 exposure (Fig. S6). In view of these observations, the absolute MAC values reported in this paper should be treated as approximate. Nonetheless, the relative extent of browning in different types of SOA should be valid because all of the experiments were conducted using the same aging protocol.

4. Discussion

4.1. Comparison of browning in different types of SOA

Table 1 and Fig. 2 show that the ΔMAC values for the OH-generated SOA are systematically lower than the corresponding values for the O_3-generated SOA. For example, ΔMAC values for LIM/O_3 SOA are almost an order of magnitude larger than for LIM/OH SOA. The same observation applies to the PIN/O_3 vs. PIN/OH pair. ISO/O_3 and ISO/OH had very low ΔMAC values, but ΔMAC was somewhat larger for the ISO/O_3 case. This observation is qualitatively consistent with the suggested role of carbonyl compounds in the browning process. We propose that the initial step in the brown carbon formation is the reaction between carbonyl groups in SOA molecules with ammonia leading to hemiaminals, which may dehydrate into primary imines (Bones et al., 2010; Laskin et al., 2010).

$$R_1R_2C{=}O + NH_3 \rightleftarrows R_1R_2C(OH)NH_2 \rightleftarrows R_1R_2C{=}NH + H_2O \quad (R1)$$
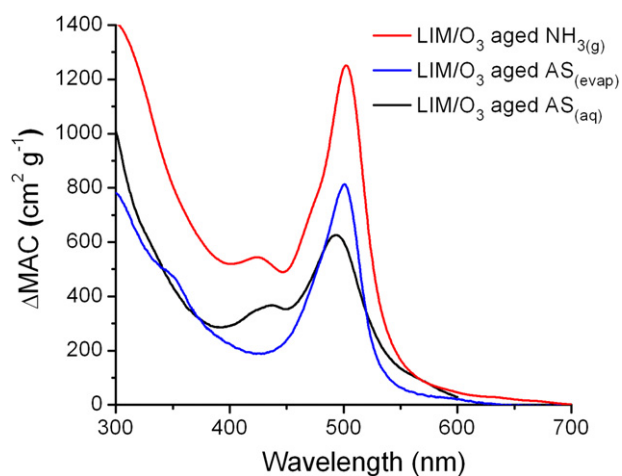
Fig. 4. Comparison of ΔMAC resulting from aging of LIM/O_3 SOA by different mechanisms: by exposure to $NH_3(g)$ (red trace), by aqueous reaction with $(NH_4)_2SO_4$ (black trace), and by evaporation of an aqueous solution of SOA mixed with $(NH_4)_2SO_4$ (blue trace). (For interpretation of the references to color in this figure legend, the reader is referred to the web version of this article.)

As mentioned in the introduction, reaction (R1) also occurs with dissolved NH_4^+, the dominant form of ammonia in atmospheric particles, over an environmentally relevant range of pH values (Bones et al., 2010; Nguyen et al., 2012). Primary imines are not stable in aqueous phase, and may react further via (R2) with another carbonyl group through nucleophilic addition initiated by one of its equilibrium forms in water, likely the hemiaminal (Amarnath et al., 1991), resulting in a more-stable secondary imine (or Schiff base):

(R2)
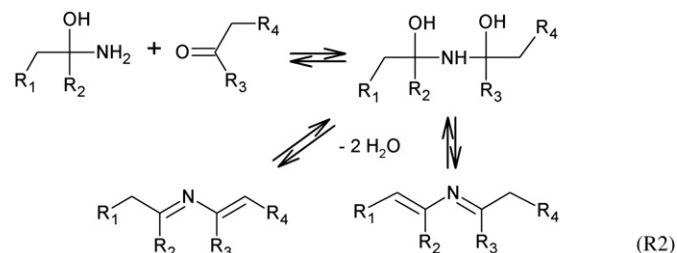
If the carbonyl group participating in reaction (R2) is part of the same molecule, a heterocyclic nitrogen-containing compound is produced. An example is the Paal-Knorr pyrrole-forming reaction (R3) between 1,4-dicarbonyls and ammonia or amines (Knorr, 1884; Paal, 1884):

(R3)
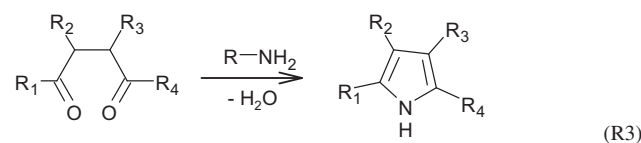
More complicated reactions involving ammonia and carbonyls are also possible. For example, 1,2-dicarbonyls react with aldehydes in the presence of ammonia through a Debus reaction (R4) leading to substituted imidazoles (De Haan et al., 2009; Debus, 1858):
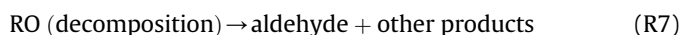

(R4)
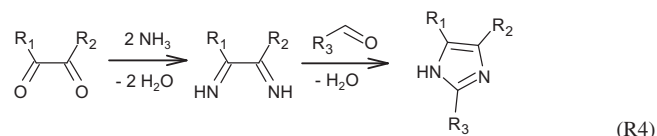
The detailed discussion of other possible reactions involving carbonyl compounds and ammonia and leading to various heterocyclic products is beyond the scope of this work. We note, however, that the cyclization (R3 and R4) and Schiff base formation (R2) reactions may produce light-absorbing products if they result in sufficient π-conjugation in the final product.

The yield of products that are both stable with respect to hydrolysis and light-absorbing is likely small; a rough estimate for LIM/O_3 is $\sim$1% (Nguyen et al., 2012). However, these minority products absorb radiation strongly enough to control MAC of SOA in the visible range of the spectrum (Nguyen et al., 2012). Carbonyls are the dominant products of the O_3-initiated oxidation of alkenes (Bailey, 1978) due to the Criegee opening of the C=C double bond. In contrast, the yields of carbonyls in the OH-initiated oxidation of terpenes tend to be smaller (Hakola et al., 1994; Jaoui and Kamens, 2003; Palen et al., 1992; Yu et al., 1999). OH reacts with alkenes primarily by addition to the C=C bond, and carbonyls can only be produced by secondary reactions of the resulting hydroxy-alkylperoxy radicals with NO. Furthermore, OH chemistry is less likely to generate dicarbonyl products; hydroxycarbonyl products are more common (Lim and Ziemann, 2009). The reduced fraction of carbonyls in VOC/OH SOA relative to VOC/O$_3$ SOA makes the

relative importance of reactions (R1–R4) smaller, and likely reduces the overall yield of stable nitrogen-containing compounds, including the light-absorbing ones.

Similar arguments may explain the effect of NO_x on ΔMAC of photooxidation SOA. For the three comparative VOC/OH/NO_x vs. VOC/OH cases studied in this work (VOC = TMB, NAP, TET), ΔMAC was reproducibly larger for the high-NO_x samples (Fig. 2). NO converts alkylperoxy radicals (RO_2) into alkyloxy radicals (RO), which form carbonyl products by direct reaction with O_2 or via decomposition (Finlayson-Pitts and Pitts, 2000).

$$NO + RO_2 \rightarrow RO + NO_2 \tag{R5a}$$

$$NO + RO_2 \rightarrow RONO_2 \tag{R5b}$$

$$RO + O_2 \rightarrow carbonyl + HO_2 \tag{R6}$$

$$RO\ (decomposition) \rightarrow aldehyde + other\ products \tag{R7}$$

For example, decomposition was important in the high-NO_x oxidation of NAP leading to a number of ring-opening products (Kautzman et al., 2010). Even if isomerization of RO by an H-shift reaction is fast, the high-NO_x chemistry that follows such an isomerization will also result in a hydroxycarbonyl product (Lim and Ziemann, 2009). In contrast, RO_2 radicals instead react with HO_2 in the NO_x-free case.

$$RO_2 + HO_2 \rightarrow alcohols, carbonyls, peroxides \tag{R8}$$
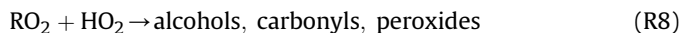
Although reaction (R8) also generates carbonyls, which can be the same ones as the high-NO_x carbonyl products, their yield is generally lower. With the smaller fraction of carbonyls in SOA under the conditions of low-NO_x OH oxidation, the yield of the stable nitrogen-containing compounds and brown carbon in SOA exposed to NH_3 should be reduced.

A distinctive feature in the spectra of aged SOA from certain biogenic precursors, such as CED/O_3, PNO/O_3, HUM/O_3, LIM/O_3 and LIM/OH, is a strong absorption band at 500 nm (Fig. 3). A similar band was also observed by Bones et al. (2010) in reactions of aqueous extracts of LIM/O_3 with AS, by Laskin et al. (2010) in reactions of LIM/O_3 with gaseous ammonia, and by Nguyen et al. (2012) in evaporated LIM/O_3 + AS solutions. The narrow width and highly reproducible peak position of this band suggests a well-defined structural motif for the chromophore and its precursor. The band appearing at ~430 nm in some of the spectra was also observed previously in aged LIM/O_3. Nguyen et al. (2012) showed that it corresponds to a different chromophore formed by an independent mechanism compared to the 500 nm absorber. It is clear that the reactions leading to this chromophore must require a rather specific distribution of functional groups in the SOA precursor molecules because this band does not appear in the spectra of other aged biogenic SOA samples: FAR/O_3, PIN/O_3, PIN/OH, ISO/O_3 and ISO/OH.

A comparison of closely-related VOC precursors in relation to the ability for their SOA to brown in the presence of NH_3 provides additional insights into the mechanism. Of the three sesquiterpenes studied here, the cyclic ones (CED and HUM) led to SOA browning, whereas the open-chain one (FAR) did not. In fact, none of the open chain VOC precursors (TET, ISO, FAR) produced SOA capable of browning. Products of oxidation of cyclic VOC tend to have a higher number of carbon atoms and should produce more dicarbonyls, which are more prone to cyclization via reactions like (R3) and (R4), leading to stable products. However, observations of the aging of PIN SOA are inconsistent with this trend. The contrast between monoterpenes PIN and LIM is especially striking; both of them have a similar endocyclic double bond, but LIM/O_3 SOA browns very efficiently whereas PIN/O_3 SOA does not. The absence of an exocyclic carbon–carbon double bond and the structural rigidity imposed by the cyclobutane ring in PIN likely contribute in varying degree to its inability to participate in reactions leading to browning that occurs readily in LIM SOA. The mechanistic differences between LIM and PIN will be discussed in a separate paper dealing with the molecular level analysis of the chromophoric products by high resolution mass spectrometry.

4.2. Comparison with field observation of brown and black carbon

Table 2 contains a compilation of recently-reported MAC values for field and lab studies of organic aerosols optical properties (Alexander et al., 2008; Bond and Bergstrom, 2006; Chakrabarty et al., 2010; Chen and Bond, 2010; Clarke et al., 2007; Dinar et al., 2008; Flowers et al., 2010; Hand et al., 2005; Kirchstetter et al., 2004; Yang et al., 2009). We focus on studies that either had no significant contributions from black carbon, the most potent radiation absorber in atmospheric particles, or explicitly removed such contributions. In cases where imaginary refractive index k was provided, it was converted into MAC using the following relationship:

$$MAC = \frac{4 \times \pi \times k}{\rho_{material} \times \lambda} \tag{5}$$

The table includes MAC values measured around 500 nm, where some of the aged VOC/O_3 SOA absorb (Fig. 3) and where solar radiation is at its peak. With the exception of data from this work, all the aerosols listed in Table 2 likely correspond to primary sources, such as biomass burning.

Table 2
Values of MAC in $m^2\ g^{-1}$ from representative field and laboratory studies of organic aerosols measured at or near 500 nm. The cited MAC values explicitly remove contributions from black carbon. With the exception of this work, all data cited in this table likely correspond to primary sources of brown carbon.

Sample (campaign)	λ (nm)	MAC ($m^2\ g^{-1}$)	Reference
Brown carbon produced by aging SOA with 100 ppb NH_3 (lab)	500	0.001–0.1	This work
"Tar balls" from smoldering combustion of wood; brown carbon contribution (lab)	532	0.01–0.07 (calculated from k = 0.0005–0.003)	(Chakrabarty et al., 2010)
HUmic-LIke Substances (HULIS) extracted from filter samples from various sites in Europe	532	0.07–1 (calculated from k = 0.003–0.05)	(Dinar et al., 2008)
Methanol extracts from wood combustion particles (lab)	500	0.1–0.5 (estimated from the graphs)	(Chen and Bond, 2010)
Refractory organic carbon from biomass burning in North America (INTEX/ICARTT)	470	0.6	(Clarke et al., 2007)
	530	0.1	
"Tar balls" in North America (YACS)	632	0.4 (calculated from reported k = 0.02)	(Hand et al., 2005)
Brown carbon in pollution plumes from Asia (CAPMEX)	532	0–1	(Flowers et al., 2010)
Brown carbon in particles collected in Asia (EAST-AIRE)	520	0.6	(Yang et al., 2009)
Acetone extracts form biomass burning aerosols in Africa (SAFARI 2010)	500	0.9	(Kirchstetter et al., 2004)
Amorphous carbon spheres from biomass burning (ACE Asia)	550	4	(Alexander et al., 2008)

The 500 nm MAC values for the secondary brown carbon studied in this work range from 10 to 1200 cm^2 g^{-1}, averaging to ~300 cm^2 g^{-1} across all the SOA listed in Table 1. This average value about two orders of magnitude smaller compared to MAC = 5×10^4–10^5 cm^2 g^{-1} for particles containing black carbon, which were collected at or near combustion sources (Bond and Bergstrom, 2006). Even higher values of MAC, well in excess of 10^5 cm^2 g^{-1}, were observed for particles composed primarily of black carbon. We conclude that in areas where black carbon accounts for at least several percent of the particulate matter by mass, brown carbon from the NH$_3$/NH$_4^+$ + SOA chemistry is not likely to be a major contributor to aerosol absorption (although it may act to amplify the black carbon effects in mixed black/brown carbon particles).

The MAC values measured in this work are comparable to MAC of organic aerosol from biomass burning (Table 2). For example, MAC = 100–700 cm^2 g^{-1} (Chakrabarty et al., 2010) and MAC = 1000–5000 cm^2 g^{-1} (Chen and Bond, 2010) were measured for acetone or methanol soluble fraction of particles produced during controlled burning of wood. Extracts of HUmic-LIke Substances (HULIS) from particles collected at various field sites had MAC = 1000–5000 cm^2 g^{-1} (Dinar et al., 2008). The MAC values for brown carbon observed in the remaining field samples listed in Table 2 vary from 1×10^3 to 4×10^4 cm^2 g^{-1}. With the NH$_3$/NH$_4^+$ + SOA brown carbon MAC values at the lower end of this range, it may have non-negligible contributions to aerosol absorption in areas that are not significantly affected by the primary emissions from the biomass burning and fossil fuel combustion. We note that such emissions are also associated with elevated levels of NO$_x$, which enhances the degree of browning in NH$_3$/NH$_4^+$ + SOA reactions and makes evaluation of the role of the NH$_3$/NH$_4^+$ + SOA brown carbon difficult.

4.3. Atmospheric implications

Most SOA produced by atmospheric oxidation of biogenic and anthropogenic precursors do no absorb visible radiation. However, certain types of SOA may become weakly absorbing as a result of reactions with reduced nitrogen compounds such as ammonia. This transformation is significant as it may potentially change the sign of the radiative forcing by SOA from negative (cooling) to positive (warming). The brown carbon aerosols studied in this work should be classified as "secondary" because they are produced directly in the atmosphere as a result of chemistry. Table 3 contrasts the properties of secondary NH$_3$/NH$_4^+$ + SOA brown carbon aerosols with those of the primary black carbon and brown carbon aerosols. Black carbon and biomass burning brown carbon are associated with primary aerosols, and start contributing to aerosol optical density as soon as they are emitted. In contrast, it may take significant time to produce NH$_3$/NH$_4^+$ + SOA brown carbon: oxidation of VOC to SOA takes hours, and reactions between SOA compounds and ammonia or AS may take days. The induction period reduces the direct radiative forcing by secondary brown carbon compounds relative to the primary light-absorbing aerosols. However, other mechanisms for producing secondary brown carbon such as evaporative cloud processing of SOA with AS may be orders of magnitude faster than the slow SOA + NH$_3$/NH$_4^+$ reaction.

A question that always arises in smog chamber studies of SOA formation and aging is to what extent the behavior of the chamber-generated SOA is representative of the real ambient aerosol. The concentrations of VOC and oxidants used in this work are considerably higher than the corresponding concentrations in the air. The role of the RO$_2$ + RO$_2$ reactions in the SOA formation may be unrealistically high as a result, especially for SOA prepared with ozone or with OH under low NO$_x$ conditions. However,

Table 3
Comparison between black carbon, primary brown carbon, and the NH$_3$/NH$_4^+$ + SOA secondary brown carbon aerosols studied in this work.

	Black carbon	Primary brown carbon	NH$_3$/NH$_4^+$ + SOA secondary brown carbon
Dominant sources	Anthropogenic	Biogenic	Biogenic
Mechanism of formation	Combustion	Biomass burning	NH$_3$ + SOA chemistry
Induction period for the appearance of light absorption	None	None	Days
Typical MAC	>10 m^2 g^{-1}	0.1–1 m^2 g^{-1}	<0.1 m^2 g^{-1}
Importance	Regional	Global	Regional

Nguyen et al. (2012) demonstrated that a two order-of-magnitude decrease in initial LIM loading in the ozonolysis reaction leading to SOA formation only diminished the MAC of the NH$_4^+$-aged SOA by 30%, suggesting that RO$_2$ + RO$_2$ chemistry has a much smaller role in generating brown carbon precursors than other reactions occurring during ozonolysis. Additionally, all SOA samples were prepared under dry conditions in this work, which are known to promote more extensive ester formation and oligomerization in particles compared to humid conditions (Nguyen et al., 2011b; Zhang et al., 2011). It would be of interest to conduct similar experiments with field samples collected from different locations for example isoprene SOA dominated Amazon forest vs. α-pinene SOA dominated boreal forest vs. urban environment to test whether the browning chemistry described in this paper occurs in actual aerosols.

The NH$_3$/NH$_4^+$ + SOA brown carbon may contribute to aerosol absorption under favorable conditions. Its formation requires significant photochemical activity necessary for conversion of VOC into SOA, and elevated concentrations of NH$_3$ in the gas phase or its ammonium salts in the particle phase necessary for generation of brown carbon. Significant changes in relative humidity should also favor brown carbon production because browning reactions are accelerated by cloud- and fog-processing of aerosols (Nguyen et al., 2012). The most likely mechanism of brown carbon formation would likely involve scavenging of SOA and AS by fog droplets or wet aerosols under humid conditions, followed by evaporation of droplets at a later time when the humidity drops. Such conditions (high concentration of reduced nitrogen compounds, frequent changes in humidity, and high photochemical activity) may exist in predominantly agricultural areas and in forested areas. In such areas, the NH$_3$/NH$_4^+$ + SOA brown carbon may potentially become the dominant contributor to aerosol absorption.

Appendix A. Supplementary material

Supplementary material related to this article can be found online at http://dx.doi.org/10.1016/j.atmosenv.2012.09.012. It includes: the structures and suppliers of all precursors used for the generation of SOA samples (Table S1); tests for the solubility of SOA samples in water and methanol (Figs. S1 and S2); tests for the completeness of SOA extraction from the filter (Fig. S3); sensitivity of the degree of browning to the substrate used for SOA collection (Fig. S4); proof that browning chemistry is not a result of impurities present in the SOA precursor (Fig. S5); time dependence for the browning process (Fig. S6).

References

Alexander, D.T.L., Crozier, P.A., Anderson, J.R., 2008. Brown carbon spheres in East Asian outflow and their optical properties. Science 321 (5890), 833–836.

Amarnath, V., Anthony, D.C., Amarnath, K., Valentine, W.M., Wetterau, L.A., Graham, D.G., 1991. Intermediates in the Paal-Knorr synthesis of pyrroles. J. Org. Chem. 56 (24), 6924–6931.

Andreae, M.O., Gelencser, A., 2006. Black carbon or brown carbon? The nature of light-absorbing carbonaceous aerosols. Atmos. Chem. Phys. 6 (10), 3131–3148.

Bailey, P.S., 1978. Organic Chemistry, Vol. 39, Pt. 1: Ozonation in Organic Chemistry, Vol. 1: Olefinic Compounds. Academic Press, 272 pp.

Bateman, A.P., Walser, M.L., Desyaterik, Y., Laskin, J., Laskin, A., Nizkorodov, S.A., 2008. The effect of solvent on the analysis of secondary organic aerosol using electrospray ionization mass spectrometry. Environ. Sci. Technol. 42 (19), 7341–7346.

Bateman, A.P., Nizkorodov, S.A., Laskin, J., Laskin, A., 2011. Photolytic processing of secondary organic aerosols dissolved in cloud droplets. Phys. Chem. Chem. Phys. 13 (26), 12199–12212.

Bond, T., Bergstrom, R., 2006. Light absorption by carbonaceous particles: an investigative review. Aerosol Sci. Technol. 40 (1), 27–67.

Bones, D.L., Henricksen, D.K., Mang, S.A., Gonsior, M., Bateman, A.P., Nguyen, T.B., Cooper, W.J., Nizkorodov, S.A., 2010. Appearance of strong absorbers and fluorophores in limonene-O_3 secondary organic aerosol due to NH_4^+-mediated chemical aging over long time scales. J. Geophys. Res. D 115 (D5), D05203. http://dx.doi.org/10.1029/2009JD012864.

Casale, M.T., Richman, A.R., Elrod, M.J., Garland, R.M., Beaver, M.R., Tolbert, M.A., 2007. Kinetics of acid-catalyzed aldol condensation reactions of aliphatic aldehydes. Atmos. Environ. 41 (29), 6212–6224.

Chakrabarty, R.K., Moosmller, H., Chen, L.W.A., Lewis, K., Arnott, W.P., Mazzoleni, C., Dubey, M.K., Wold, C.E., Hao, W.M., Kreidenweis, S.M., 2010. Brown carbon in tar balls from smoldering biomass combustion. Atmos. Chem. Phys. 10 (13), 6363–6370.

Chang, J.L., Thompson, J.E., 2010. Characterization of colored products formed during irradiation of aqueous solutions containing H_2O_2 and phenolic compounds. Atmos. Environ. 44 (4), 541–551.

Chen, Y., Bond, T.C., 2010. Light absorption by organic carbon from wood combustion. Atmos. Chem. Phys. 10 (4), 1773–1787.

Clarke, A., McNaughton, C., Kapustin, V., Shinozuka, Y., Howell, S., Dibb, J., Zhou, J., Anderson, B., Brekhovskikh, V., Turner, H., Pinkerton, M., 2007. Biomass burning and pollution aerosol over North America: organic components and their influence on spectral optical properties and humidification response. J. Geophys. Res. D 112 (D12), D12S18. http://dx.doi.org/10.1029/2006JD007777.

Clegg, S.L., Brimblecombe, P., Wexler, A.S., 1998. Thermodynamic model of the system $H^+–NH_4^+–SO_4^{2-}–NO_3^-–H_2O$ at tropospheric temperatures. J. Phys. Chem. A 102 (12), 2137–2154.

De Haan, D.O., Corrigan, A.L., Smith, K.W., Stroik, D.R., Turley, J.J., Lee, F.E., Tolbert, M.A., Jimenez, J.L., Cordova, K.E., Ferrell, G.R., 2009. Secondary organic aerosol-forming reactions of glyoxal with amino acids. Environ. Sci. Technol. 43 (8), 2818–2824.

Debus, H., 1858. Ueber die Einwirkung des Ammoniaks auf Glyoxal. Justus Liebigs Ann. Chem. 107 (2), 199–208.

Dinar, E., Abo Riziq, A., Spindler, C., Erlick, C., Kiss, G., Rudich, Y., 2008. The complex refractive index of atmospheric and model humic-like substances (HULIS) retrieved by a cavity ring down aerosol spectrometer (CRD-AS). Faraday Discuss. 137, 279–295.

Esteve, W., Noziere, B., 2005. Uptake and reaction kinetics of acetone, 2-butanone, 2,4-pentanedione, and acetaldehyde in sulfuric acid solutions. J. Phys. Chem. A 109 (48), 10920–10928.

Finlayson-Pitts, B.J., Pitts, J.N., 2000. Chemistry of the Upper and Lower Atmosphere: Theory, Experiments, and Applications. Academic Press, San Diego, 1040 pp.

Flowers, B.A., Dubey, M.K., Mazzoleni, C., Stone, E.A., Schauer, J.J., Kim, S.W., Yoon, S.C., 2010. Optical–chemical–microphysical relationships and closure studies for mixed carbonaceous aerosols observed at Jeju Island; 3-laser photoacoustic spectrometer, particle sizing, and filter analysis. Atmos. Chem. Phys. 10 (21), 10387–10398.

Galloway, M.M., Chhabra, P.S., Chan, A.W.H., Surratt, J.D., Flagan, R.C., Seinfeld, J.H., Keutsch, F.N., 2009. Glyoxal uptake on ammonium sulphate seed aerosol: reaction products and reversibility of uptake under dark and irradiated conditions. Atmos. Chem. Phys. 9 (10), 3331–3345.

Garland, R.M., Elrod, M.J., Kincaid, K., Beaver, M.R., Jimenez, J.L., Tolbert, M.A., 2006. Acid-catalyzed reactions of hexanal on sulfuric acid particles: identification of reaction products. Atmos. Environ. 40 (35), 6863–6878.

Gelencser, A., Hoffer, A., Kiss, G., Tombacz, E., Kurdi, R., Bencze, L., 2003. In-situ formation of light-absorbing organic matter in cloud water. J. Atmos. Chem. 45 (1), 25–33.

Hakola, H., Arey, J., Aschmann, S.M., Atkinson, R., 1994. Product formation from the gas-phase reactions of OH radicals and O_3 with a series of monoterpenes. J. Atmos. Chem. 18 (1), 75–102.

Hand, J.L., Malm, W.C., Laskin, A., Day, D., Lee, T., Wang, C., Carrico, C., Carrillo, J., Cowin, J.P., Collett Jr., J., Iedema, M.J., 2005. Optical, physical, and chemical properties of tar balls observed during the Yosemite aerosol characterization study. J. Geophys. Res. D 110 (D21), D21210. http://dx.doi.org/10.1029/2004JD005728.

Haywood, J., Boucher, O., 2000. Estimates of the direct and indirect radiative forcing due to tropospheric aerosols: a review. Rev. Geophys. 38 (4), 513–543.

Hoffer, A., Kiss, G., Blazso, M., Gelencser, A., 2004. Chemical characterization of humic-like substances (HULIS) formed from a lignin-type precursor in model cloud water. Geophys. Res. Lett. 31 (6), L06115. http://dx.doi.org/10.1029/2003GL018962.

Jacobson, M.Z., 1999. Isolating nitrated and aromatic aerosols and nitrated aromatic gases as sources of ultraviolet light absorption. J. Geophys. Res. D 104 (D3), 3527–3542. http://dx.doi.org/10.1029/1998JD100054.

Jaoui, M., Kamens, R.M., 2003. Mass balance of gaseous and particulate products from beta-pinene/O_3/air in the absence of light and beta-pinene/NO_x/air in the presence of natural sunlight. J. Atmos. Chem. 45 (2), 101–141.

Jaoui, M., Edney, E.O., Kleindienst, T.E., Lewandowski, M., Offenberg, J.H., Surratt, J.D., Seinfeld, J.H., 2008. Formation of secondary organic aerosol from irradiated α-pinene/toluene/NO_x mixtures and the effect of isoprene and sulfur dioxide. J. Geophys. Res. D 113 (D9), D09303. http://dx.doi.org/10.1029/2007JD009426.

Kautzman, K.E., Surratt, J.D., Chan, M.N., Chan, A.W.H., Hersey, S.P., Chhabra, P.S., Dalleska, N.F., Wennberg, P.O., Flagan, R.C., Seinfeld, J.H., 2010. Chemical composition of gas- and aerosol-phase products from the photooxidation of naphthalene. J. Phys. Chem. A 114 (2), 913–934.

Kirchstetter, T.W., Novakov, T., Hobbs, P.V., 2004. Evidence that the spectral dependence of light absorption by aerosols is affected by organic carbon. J. Geophys. Res. D 109 (D21), D21208. http://dx.doi.org/10.1029/2004JD004999.

Knorr, L., 1884. Synthese von Furfuranderivaten aus dem Diacetbernsteinsäureester. Ber. Dtsch. Chem. Ges. 17 (2), 2863–2870.

Krizner, H.E., De Haan, D.O., Kua, J., 2009. Thermodynamics and kinetics of methylglyoxal dimer formation: a computational study. J. Phys. Chem. A 113 (25), 6994–7001.

Kwamena, N.O.A., Abbatt, J.P.D., 2008. Heterogeneous nitration reactions of polycyclic aromatic hydrocarbons and n-hexane soot by exposure to NO_3/NO_2/N_2O_5. Atmos. Environ. 42 (35), 8309–8314.

Laskin, J., Laskin, A., Roach, P.J., Slysz, G.W., Anderson, G.A., Nizkorodov, S.A., Bones, D.L., Nguyen, L.Q., 2010. High-resolution desorption electrospray ionization mass spectrometry for chemical characterization of organic aerosols. Analyt. Chem. 82 (5), 2048–2058.

Lim, Y.B., Ziemann, P.J., 2009. Chemistry of secondary organic aerosol formation from OH radical-initiated reactions of linear, branched, and cyclic alkanes in the presence of NO_x. Aerosol Sci. Technol. 43 (6), 604–619.

Limbeck, A., Kulmala, M., Puxbaum, H., 2003. Secondary organic aerosol formation in the atmosphere via heterogeneous reaction of gaseous isoprene on acidic particles. Geophys. Res. Lett. 30 (19), 1996. http://dx.doi.org/10.1029/2003GL017738.

Nguyen, T.B., Laskin, J., Laskin, A., Nizkorodov, S.A., 2011a. Nitrogen-containing organic compounds and oligomers in secondary organic aerosol formed by photooxidation of isoprene. Environ. Sci. Technol. 45 (16), 6908–6918.

Nguyen, T.B., Roach, P.J.L., Laskin, J.A., Nizkorodov, S.A., 2011b. Effect of humidity on the composition of isoprene photooxidation secondary organic aerosol. Atmos. Chem. Phys. 11, 6931–6944.

Nguyen, T.B., Lee, P.B., Updyke, K.M., Bones, D.L., Laskin, J., Laskin, A., Nizkorodov, S.A., 2012. Formation of nitrogen- and sulfur-containing light-absorbing compounds accelerated by evaporation of water from secondary organic aerosols. J. Geophys. Res. D 117, D01207. http://dx.doi.org/10.1029/2011JD016944.

Noziere, B., Esteve, W., 2005. Organic reactions increasing the absorption index of atmospheric sulfuric acid aerosols. Geophys. Res. Lett. 32 (3), L03812. http://dx.doi.org/10.1029/2004GL021942.

Noziere, B., Esteve, W., 2007. Light-absorbing aldol condensation products in acidic aerosols: spectra, kinetics, and contribution to the absorption index. Atmos. Environ. 41 (6), 1150–1163.

Noziere, B., Voisin, D., Longfellow, C.A., Friedli, H., Henry, B.E., Hanson, D.R., 2006. The Uptake of methyl vinyl ketone, methacrolein, and 2-methyl-3-butene-2-ol onto sulfuric acid solutions. J. Phys. Chem. A 110 (7), 2387–2395.

Noziere, B., Dziedzic, P., Cordova, A., 2009. Products and kinetics of the liquid-phase reaction of glyoxal catalyzed by ammonium ions (NH_4^+). J. Phys. Chem. A 113 (1), 231–237.

Paal, C., 1884. Ueber die Derivate des Acetophenonacetessigesters und des Acetonylacetessigesters. Ber. Dtsch. Chem. Ges. 17 (2), 2756–2767.

Palen, E.J., Allen, D.T., Pandis, S.N., Paulson, S.E., Seinfeld, J.H., Flagan, R.C., 1992. Fourier transform infrared analysis of aerosol formed in the photo-oxidation of isoprene and beta -pinene. Atmos. Environ. 26A (7), 1239–1251.

Pitts Jr., J.N., Van Cauwenberghe, K.A., Grosjean, D., Schmid, J.P., Fitz, D.R., Belser Jr., W.L., Knudson, G.B., Hynds, P.M., 1978. Atmospheric reactions of polycyclic aromatic hydrocarbons: facile formation of mutagenic nitro derivatives. Science 4367, 515–519.

Ramanathan, V., Ramana, M.V., Roberts, G., Kim, D., Corrigan, C., Chung, C., Winker, D., 2007. Warming trends in Asia amplified by brown cloud solar absorption. Nature 448 (7153), 575–578.

Rincon, A.G., Guzmán, M.I., Hoffmann, M.R., Colussi, A.J., 2009. Optical absorptivity versus molecular composition of model organic aerosol matter. J. Phys. Chem. A 113 (39), 10512–10520.

Rincon, A.G., Guzmán, M.I., Hoffmann, M.R., Colussi, A.J., 2010. Thermochromism of model organic aerosol matter. J. Phys. Chem. Lett. 1 (1), 368–373.

Sareen, N., Schwier, A.N., Shapiro, E.L., Mitroo, D., McNeill, V.F., 2010. Secondary organic material formed by methylglyoxal in aqueous aerosol mimics. Atmos. Chem. Phys. 10 (3), 997–1016.

Shapiro, E.L., Szprengiel, J., Sareen, N., Jen, C.N., Giordano, M.R., McNeill, V.F., 2009. Light-absorbing secondary organic material formed by glyoxal in aqueous aerosol mimics. Atmos. Chem. Phys. 9 (7), 2289–2300.

Solomon, S., Qin, D., Manning, M., Chen, Z., Marquis, M., Averyt, K.B., Tignor, M., Miller, H.L., 2007. Climate Change 2007: the Physical Science Basis. In: Contribution of Working Group I to the Fourth Assessment Report of the Intergovernmental Panel on Climate Change. Cambridge University Press, Cambridge, UK and New York, USA, 996 pp.

Trainic, M., Abo Riziq, A., Lavi, A., Flores, J.M., Rudich, Y., 2011. The optical, physical and chemical properties of the products of glyoxal uptake on ammonium sulfate seed aerosols. Atmos. Chem. Phys. 11 (18), 9697–9707.

Usher, C.R., Michel, A.E., Grassian, V.H., 2003. Reactions on mineral dust. Chem. Rev. 103 (12), 4883–4939.

Walser, M.L., Desyaterik, Y., Laskin, J., Laskin, A., Nizkorodov, S.A., 2008. High-resolution mass spectrometric analysis of secondary organic aerosol produced by ozonation of limonene. Phys. Chem. Chem. Phys. 10 (7), 1009–1022.

Yang, M., Howell, S.G., Zhuang, J., Huebert, B.J., 2009. Attribution of aerosol light absorption to black carbon, brown carbon, and dust in China – interpretations of atmospheric measurements during EAST-AIRE. Atmos. Chem. Phys. 9 (6), 2035–2050.

Yu, J., Cocker III, D.R., Griffin, R.J., Flagan, R.C., Seinfeld, J.H., 1999. Gas-phase ozone oxidation of monoterpenes: gaseous and particulate products. J. Atmos. Chem. 34 (2), 207–258.

Yu, G., Bayer, A.R., Galloway, M.M., Korshavn, K.J., Fry, C.G., Keutsch, F.N., 2011. Glyoxal in aqueous ammonium sulfate solutions: products, kinetics and hydration effects. Environ. Sci. Technol. 45 (15), 6336–6342.

Zhang, H., Surratt, J.D., Lin, Y.H., Bapat, J., Kamens, R.M., 2011. Effect of relative humidity on SOA formation from isoprene/NO photooxidation: enhancement of 2-methylglyceric acid and its corresponding oligoesters under dry conditions. Atmos. Chem. Phys. 11 (13), 6411–6424.

Zhao, J., Levitt, N.P., Zhang, R., 2005. Heterogeneous chemistry of octanal and 2,4-hexadienal with sulfuric acid. Geophys. Res. Lett. 32 (9), L09802. http://dx.doi.org/10.1029/2004GL022200.